Modelling Hotspots in thin films using the Boltzmann Transport Equation

Aalok Gaitonde, Yash Ganatra, Bhagyashree Ganore

Purdue University, West Lafayette, IN-47906

gaitonde@purdue.edu

yganatra@purdue.edu

bganore@purdue.edu

Abstract— **Non-continuum transport models are used when the characteristic device dimension is comparable to the phonon mean free path. The need to reduce size of electronic devices has resulted in localized heat generation. When the thickness of the thin films is smaller than mean free path of phonons, non-continuum transport models are needed to model the temperature jump observed. In this project, Boltzmann transport equation (BTE) is solved in COMSOL using the built in radiative transport equation (RTE) module. The module is validated using for specular/diffusive and thermalizing boundary conditions and extended to model local hotspots.**

I. INTRODUCTION

Conduction heat transfer in the continuum model has classically been explained with help of an energy balance coupled with Fourier's law for thermal conduction. This model was very useful while modelling diffusive heat conduction. However, Fourier law cannot predict heat transfer at device lengths comparable to the mean free path of the thermal energy carriers. It is inadequate since the law assumes that heat propagates at infinite speed, and it does not differentiate between the cause and effect relationship between heat flux and a temperature gradient [1],[2]

A transistor is a semiconductor device used to amplify or switch electronic signals and electrical power. It is composed of semiconductor material with at least three terminals for connection to an external circuit. A voltage or current applied to one pair of the transistor's terminals changes the current through another pair of terminals. A cross section through a MOSFET is shown in Figure 1. When the gate voltage V_{GS} is below the threshold for making a conductive channel; there is little or no conduction between the terminals drain and source; the switch is off. When the gate is more positive, it attracts electrons, inducing an *n*-type conductive channel in the substrate below the oxide, which allows electrons to flow between the *n*-doped terminals; the switch is on.

The extreme miniaturization of transistor feature sizes in accordance with the Moore's Law, has resulted in localized heat generation. When phonons are considered as dominant thermal energy carriers, the BTE in relaxation time approximation is used to study the ballistic-diffusive thermal transport across transistor chips [2]. The emerging transistors are basically nanoscale silicon semiconductor devices with thermal transport dominated by phonons. These phonons have a mean free path of approximately 300 nm at room temperature. The device length of transistors is comparable to the phonon mean free path in silicon. The phonon wavelength which is around 5 nm is also comparable to the device lengths of the transistors [3].It should be noted that, phonon transport is ballistic if the mean free path is comparable to the device length. In other words it can be approximated that the bulk scattering events occur less frequently in smaller device lengths which are comparable to the mean free paths of the carriers. Conversely, small device lengths also increase surface to volume ratios and boundary scattering becomes important [4] . The relaxation rate described in detail further, relies heavily on how different scattering mechanisms are considered. Generally, when phonon dominated heat flow in thin films is studied, phonons are considered to get scattered by boundaries, impurities, and other phonons (Normal and Umklapp Scattering) [5]. These different scattering mechanisms are explained in detail in the sections ahead. Amongst some of the alternatives of solving this problem in thin films, the BTE equation is a tool to model the nanoscale heat transfer in thin films which takes into account the ballistic nature of phonons.

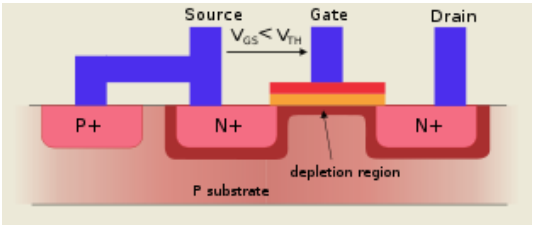

Figure 1 Schematic of a transistor [6]

This paper uses COMSOL – a commercial FEA solver to solve the BTE exploiting the analogy between the RTE and BTE [7]. The built-in RTE module is validated against two test cases and extended to model (steady state) local hotspots with prescribed temperature boundary conditions.

II. MODEL FORMULATION

A. BTE Equation in terms of distribution function:

The 3-D integral-differential equation which gives the spatial and temporal dependence of the local phonon density function $n(\mathbf{r}, \mathbf{p}, t)$, in terms of the diffusion and scattering effects is given by [8]

$$\frac{\partial \eta}{\partial t}(r,p,t) + v\nabla_r \eta(r,p,t) + \frac{F}{m}\nabla_v \eta(r,p,t) = \left[\frac{\partial \eta}{\partial t}\right]_C \quad (1)$$

where **r** and **p** are the space coordinates and momentum of the particle under consideration.

The first term is the time dependence of distribution function, the second term is the spatial distribution variation, and the third term is the forces acting on the particles. According to the Debye approximation, the group velocity of phonons does not change over a large frequency range. Hence we neglect the term with acceleration, which is ∇_v.

B. Relaxation Time Approximation

Due to the complexity of integral-differential Boltzmann equation it is difficult to solve. One of the simplifications of the scattering integral by the relaxation time approximation is given by,

$$\left[\frac{\partial \eta}{\partial t}\right]_C = -\frac{\eta^o - \eta}{\tau} \quad (2)$$

Relaxation time τ can be explained as the time taken for a non equilibrium system to relax to an equilibrium distribution.

Scattering is be caused by the presence of various processes such as boundary, defect, phonon-phonon etc. For every individual scattering process, a relaxation time can be defined. The total relaxation time, τ can be calculated from individual relaxation times according to the Matthiessen's rule:

$$\frac{1}{\Gamma_f} = \sum_j \frac{1}{\Gamma_j} \quad (3)$$

C. Phonon Scattering Mechanisms

Boundary scattering rate is given by the following equation,

$$\Gamma_B^{-1} = \frac{v}{L\,F} \quad (4)$$

where *v* is the phonon group velocity, *L* is the dimension of the sample and *F* is a geometric fitting parameter which also depends on the smoothness of the boundary.

Phonon-phonon scattering mainly is caused by into 2 types of processes, Normal processes and Umklapp processes. N processes do not impede phonon momentum and do not impede heat flow directly. They affect heat flow by re-distributing phonon energies. Umklapp processes do impede phonon momentum and hence impede heat flow. They dominate thermal conductivity of semiconductors and insulators. The Umklapp scattering is given by,

$$\Gamma_U^{-1} = \frac{\theta_{D}\,\omega}{A\,T}\, e^{\frac{-\theta_D}{\gamma T}} \quad (5)$$

A is a dimensionless constant that depends on atomic mass, lattice spacing, and Gruneisen constant. γ is a parameter that represents crystal structure [5].

Impurity scattering is caused by defects, dislocations, and boundaries change the spring constant of the lattice. A discontinuity in the lattice properties will cause a wave to alter direction or in other words scatter. Carriers with very long wavelengths relative to defect size do not easily 'feel' the defects. But carriers with shorter wavelengths will feel the defects easily and scatter.

D. Equation of Phonon Radiative Transport: EPRT

The Equation for Phonon Radiative Transport (EPRT) is derived from the BTE is used to study phonon transport in thin films. Majumdar et. Al [7] proved that the EPRT is analogous to the Radiative transport equation (RTE). They calculated the temperature distribution and heat flux in a 1-D thin film and showed that EPRT can finely accommodate the particle nature of phonons in sub-continuum spatial and time scales. Keeping in mind the integral-differential formulation of the BTE which makes it very difficult to solve, the analogy between the EPRT and the RTE has opened several ways of approaching the solution which were originally developed to solve the RTE. For a one dimensional case (thin films), the BTE can be expressed as:

$$\frac{\partial \eta}{\partial t} + v_x \frac{\partial \eta}{\partial x} = \frac{\eta^o - \eta}{\tau} \quad (6)$$

where η is the phonon distribution function
η^o is the phonon distribution in thermal equilibrium
v_x is the phonon group velocity in the x-direction
τ is the relaxation time

The differential phonon intensity dI, along a ray can be written as

$$dI(x,\theta,\phi,\omega,t) = \sum_p I_\omega\, d\omega\, d\,\Omega \quad (7)$$

The phonon intensity per unit frequency interval around ω, with spectral distribution function η per unit solid angle in the direction of phonon propagation in an isotropic medium I_ω can be given as,

$$I_\omega(\theta,\phi,\omega,x,t) = \sum_p v(\theta,\phi) n_\omega(x,t,\omega,T)\hbar\omega \frac{D(\omega)}{4\pi} \quad (8)$$

v is the phonon group velocity in the (θ, ϕ) direction

n_ω is the spectral phonon distribution for frequency around ω
$\hbar\omega$ is the energy quantum of a phonon
$D(\omega)$ is the density of state at the lattice wave of frequency ω
p is the polarization index

The Boltzmann transport equation for the spectral phonon distribution η can now be expressed in terms of spectral phonon intensity I_ω as,

$$\frac{\partial I_\omega}{\partial t} + v\mu\frac{\partial I_\omega}{\partial x} = \frac{I_\omega^o - I_\omega}{\tau} \tag{9}$$

I_ω is the spectral phonon intensity at frequency ω
v is the phonon group velocity of propagation
$\mu = \cos(\theta)$ is the direction cosine in the x-direction
τ is the relaxation time for phonon scattering in the medium

This is known as the Equation of Phonon Radiative Transport (EPRT). For steady-state conditions, EPRT can be written as,

$$v\mu\frac{\partial I_\omega}{\partial x} = \frac{I_\omega^o - I_\omega}{\tau} \tag{10}$$

The mean free path, Λ is given by,

$$\Lambda = v\,\tau$$

E. Gray body approximation:

Furthermore, if we multiply relaxation time on both sides of the steady state EPRT, and using mean free path definition, we get,

$$\Lambda\mu\frac{\partial I_\omega}{\partial x} = I_\omega^o - I_\omega \tag{11}$$

The relaxation time and phonon group velocity are independent of the phonon frequency if we assume the medium to be gray. Hence, the total phonon intensity for a gray medium can be derived as,

$$I(x) = \int_0^{\omega_D} I_\omega d\omega \tag{12}$$

The steady state EPRT for phonon intensity in the x-direction for a gray medium can be given as,

$$\Lambda\mu\frac{\partial I}{\partial x} = I^o - I \tag{13}$$

$$I^o = \frac{1}{4\pi}\int_{\Omega=4\pi} I(\mu)d\,\Omega = \frac{1}{2}\int_{-1}^{1} I(\mu)\,d\mu \tag{14}$$

and the heat flux can be derived as,

$$q_x(x) = \int_{\Omega=4\pi} \mu I\, d\Omega \tag{15}$$

F. Non dimensional form of the BTE

Nondimensionalizing (11) using

$$t^* = \frac{t}{\tau_o}$$

$$\eta = \frac{x}{L}$$

$$Kn = \frac{\Lambda}{L}$$

we get,

$$Kn\,\mu\frac{\partial I}{\partial \eta} = I_o - I \tag{16}$$

Further, applying Dirichlet Boundary Conditions we get, [9]

$$I_{\eta=0} = \frac{4\pi T_{left}}{C_v v_{g,ave}}_{\eta=0}$$

$$I_{\eta=1} = \frac{4\pi T_{right}}{C_v v_{g,ave}}_{\eta=1}$$

G. Discrete Ordinates Method

This method is used to solve for a function which is integrated over a set of n different directions as given below,

$$\int_{\Omega=4\pi} f(\hat{s})d\Omega = \sum_{i=1}^{n} w_i\ f(\hat{s}_i) \tag{17}$$

where the w_i are the quadrature weights associated with the directions $\hat{s}_i$ [10]. The quadrature can be chosen arbitrarily, although there are some restrictions on the directions and weights that come up from the desire to preserve symmetry and satisfy certain conditions. The directions and weights chosen should be completely symmetric (i.e., sets that are invariant after any rotation of 90°) and should satisfy the zeroth, first, and second moments as given below,

$$\int_{\Omega=4\pi} d\Omega = 4\pi = \sum_{i=1}^{n} w_i$$

$$\int_{\Omega=4\pi} \hat{s}d\Omega = 0 = \sum_{i=1}^{n} w_i\,\hat{s}_i$$

$$\int_{\Omega=4\pi} \hat{s}\,\hat{s}\,d\Omega = \frac{4\pi}{3}\delta = \sum_{i=1}^{n} w_i\,\hat{s}_i\hat{s}_i$$

where δ is the unit tensor. Various sets of directions and weights which satisfy each of the above given criteria have been tabulated by Lee [11] and Lathrop and Carlson [12]. It has been observed by Fiveland [13] and Truelove [14] that different sets of directions and weights may alter the accuracy of the solution considerably.

.

III. METHODOLOGY

1D steady state BTE can be extended to 2D as shown

$$Kn\left[\mu\frac{\partial I_\omega}{\partial x^*}+\eta\frac{\partial I_\omega}{\partial y^*}\right]=I_{\omega 0}-I_\omega \qquad (18)$$

where $I_{\omega 0}$ is written using the Discrete Ordinates method (DOM) described in the previous section. The general form of radiation transport equation (RTE) solved in COMSOL is [15]

$$\Omega\cdot\nabla \mathrm{I}(\Omega)=\kappa I_b(T)-\beta I(\Omega,s)+\frac{\sigma_s}{4\pi}\int_0^{4\pi} I(\Omega)\phi(\Omega',\Omega)\partial\Omega' \quad (19)$$

where I(Ω) is the radiative intensity at a given position following the Ω direction, and κ, β and σ_s are the absorption, extinction and scattering coefficients respectively. Ω is the solid angle and $\phi(\Omega',\Omega)$ is the phase function, and is taken as 1 for an isotropic material

Table 1 shows the coefficients of RTE obtained after comparing with the dimensional form of the 2D BTE.

Table 1 Comparison of coefficients of 2D BTE and RTE in COMSOL

κ	β	σ_s
0	$1/\Lambda$	$1/\Lambda$

The computational model to study the effect of hotspots is developed from a bottom up approach. The first two cases (Case A and Case B) validated the COMSOL model against a rectangular domain with the following two conditions.
Case A: Prescribed temperatures on left and right walls and specular or diffuse boundary conditions
Case B (Figure 3): Thermalizing boundary conditions - prescribed temperature on all edges (top edge at a higher temperature T_H than others which are set at the same temperatureT_C. (L/H = 2)
Case C (Figure 4): The hotspot is modelled as a Dirichlet boundary with temperature T_H on a fraction of the rectangular domain with other edges maintained at fixed lower temperature T_C .

COMSOL discretizes the equation in the angular direction using the Discrete Ordinates method described in the previous section. COMSOL discretizes a 2D geometry in S_2, S_4, S_6, S_8 angular directions which has 4,12,24,40 Gaussian quadrature points ($S_N=\frac{N(N+2)}{2}$) . Fully Coupled solver in COMSOL with a relative tolerance of 1e-3 and a tolerance factor of 1e-3 to increase the stability of the solution since it's a nonlinear problem. The material properties are shown in Table 2

Table 2 Material Properties of Si

C_v	$J/(m\text{^}3\ K)$	7e5
$v_{g,ave}$	m/s	6300

A. *Case A*

Figure 2 represents a 2D domain with two thermalizing boundaries, and two adiabatic specular or diffuse boundaries. If the mean free path of phonon is of the order of magnitude of the surface roughness of the boundary, the boundary is 'diffuse', and if the order of magnitude of the mean free path is much higher than the surface roughness, the boundary acts as a 'specular' boundary. A specular boundary does not impede heat transport, where as a diffuse boundary does.

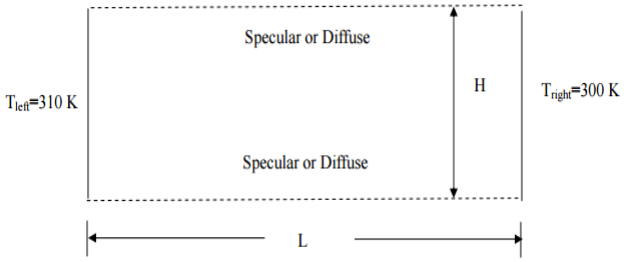

Figure 2: Schematic of boundary conditions for Case A

B. *Case B*

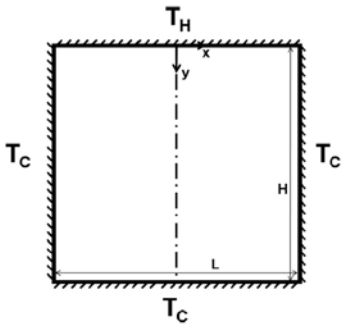

Figure 3: Schematic of boundary conditions for Case B

Figure 3 shows the boundary conditions for Case B. The effect of Knudsen number on transport regimes (ballistic, non-equilibrium and diffusive) is studied by sweeping through Kn from 0.001 to 10. The effect of angular discretization is also studied for S_2, S_4, S_6, S_8 angular directions.

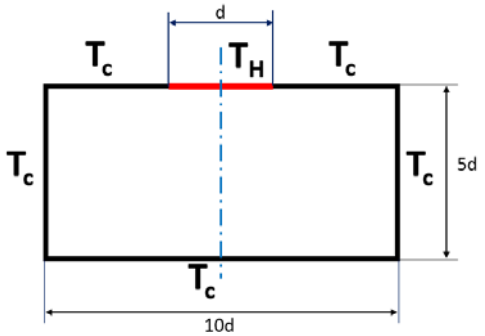

Figure 4 Schematic of local heating due to a hotspot for Case C

IV. RESULTS AND DISCUSSION

A. Case A

For a specular boundaries, and at Kn=0.1, transport is analogous to the Fourier Limit and is diffusive, and no temperature jump is seen at the boundaries, unlike for ballistic transport, for higher Kn where phonons may pass through without scattering for higher Kn (Kn > 10).

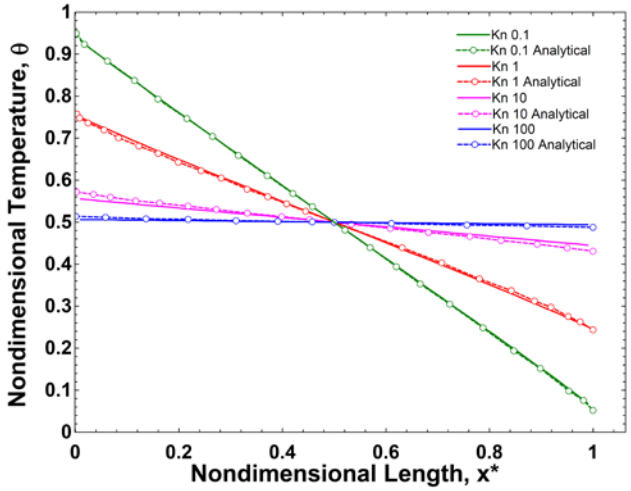

Figure 5 Comparison of non-dimensional temperature along horizontal centreline for different Kn with the analytical solution for specular boundary condition

Also, for specular boundaries, the solution behaves like a 1D problem, and there is good agreement with the analytical solution obtained by using an analogy to the radiation heat transfer [4]

$$2e_o^*(\eta) = E_2(\eta) + \int_0^{\zeta} e_o^*(\eta')\, E_1(|\eta - \eta'|)d\eta'$$

where $\eta = x/L$ is the nondimensional length, $E_n(x) = \int_0^1 \mu^{n-2} \exp\left(-\frac{x}{\mu}\right) d\mu$ is the exponential integral, ζ is the optical thickness, i.e an inverse of the Knudsen number, Kn, $e_o^*(\eta) = \frac{e_o\,(\eta) - J_{q1}^+}{J_{q1}^+ - J_{q2}^+}$ is the nondimensional emissive power at both ends of the domain.

For diffuse boundary condition as shown in Figure 6, the solution is insensitive to changes in acoustic thickness since diffuse scattering is directional independent.

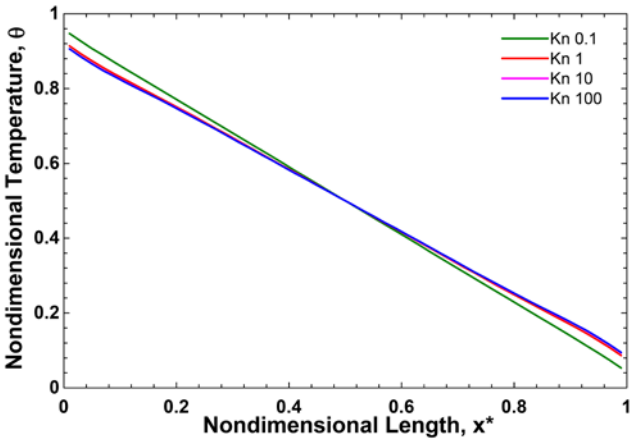

Figure 6 Variation of non-dimensional temperature along horizontal centreline for different Kn for diffuse boundary condition

B. Case B

Figure 7 shows the effects of Kn on transport regimes for a range of Kn from 0.01 to 10 for S_8 angular directions(40 quadrature points).

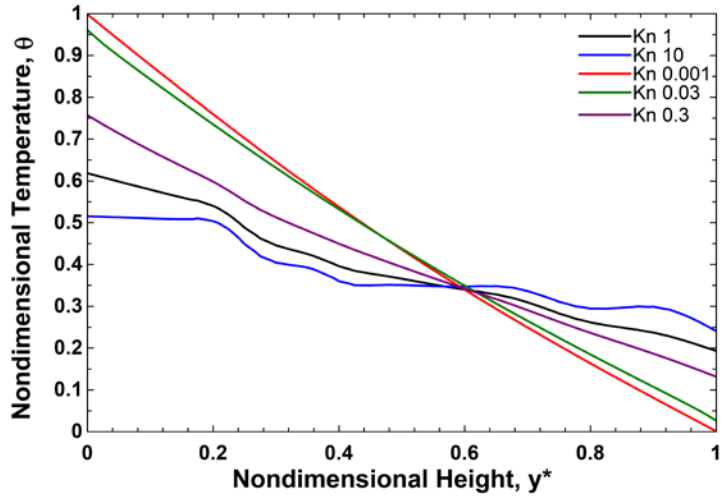

Figure 7 Variation of non-dimensional temperature along vertical centreline for different Kn for thermalizing boundary condition

The trends of Kn are similar to Figure 5 and Figure 6. For Kn = 0.001, the transport is mostly dominated by diffusive scattering without any temperature discontinuity at the boundaries. As Kn increases the transport is ballistic.

Grid independence

The variation of non-dimensional temperature is evaluated for two grids - 40 x 40 and 25 x 25 domain elements and shown in Figure 8. There is no significant variation in the results and for subsequent computations 25 x 25 grid is chosen.

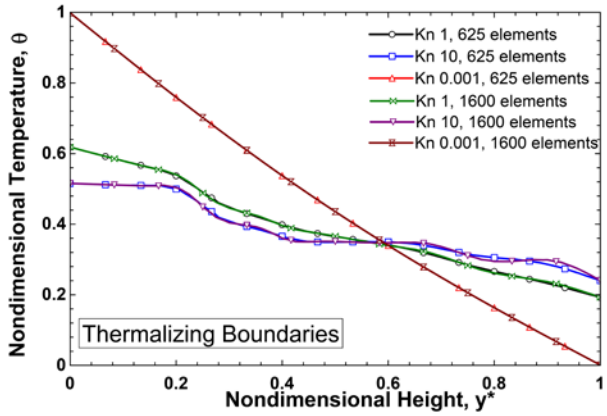

Figure 8 Grid independence test

Angular refinement – Ray Effect

The effect of increasing the Gaussian quadrature points is shown in Figure 8. With increasing angular discretization, sharp changes in temperature (at $y^* \sim 0.4$) reduce thus improving the numerical stability of the solution.

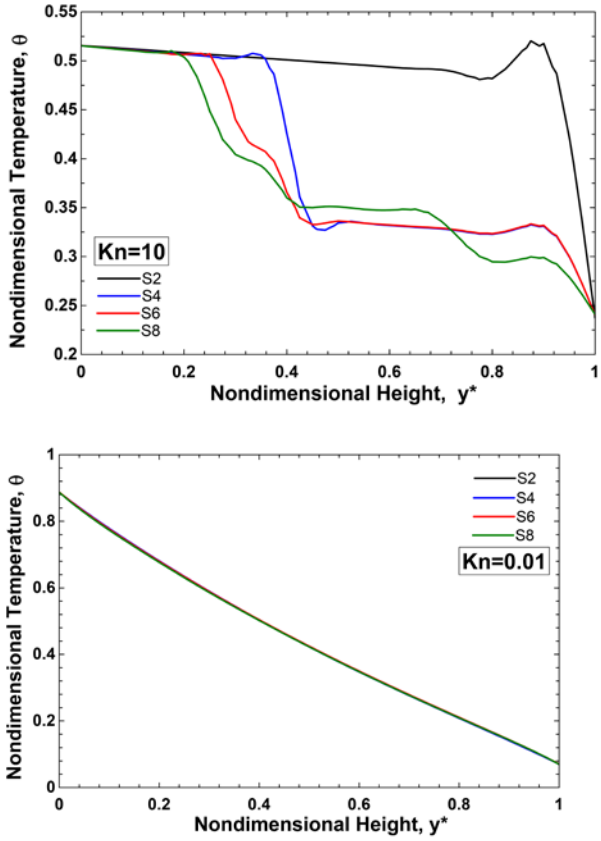

Figure 9 Effect of angular domain discretization on accuracy of BTE solution for (a) Kn = 10 (b) Kn = 0.01

Figure 9 shows the contours to highlight the effect of increasing angular discretization for Kn = 10. From Figures Figure 8, Figure 9 it can be seen that spatial and angular refinement are independent of each other. Hence using a highly refined spatial mesh with coarse angular mesh is not recommended due to the ray effect.

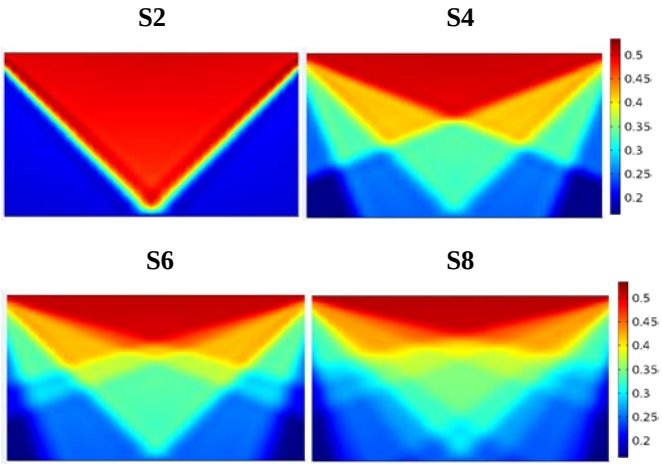

Figure 10 Effect of angular discretization for Kn = 10

C. *Case C*

To resolve the temperature gradients near the hotspot, a boundary layer mesh is used. The heat source is modelled as shown in Figure 4 to study the effect of local hotspots. The characteristic length for calculating the Knudsen number is taken as the size (length) of the hotspot (100nm in this case). The device length above which continuum transport (Fourier's law) holds can be estimated from Figure 11. For a mean free path of Si of 260 nm at 300 K [16], continuum transport can be used if the device length is of the order of $10\mu m$ at least. The mean free path of Si can be calculated from the Mattheisen's rule discussed earlier. Figure 12 shows the steady state temperature profile of a single hotspot in a silicon chip for diffusive and ballistic regimes.

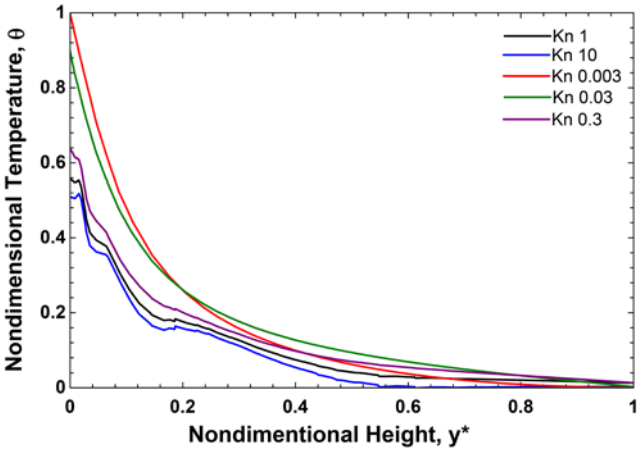

Figure 11 Variation of non-dimensional temperature along vertical centreline for different Kn

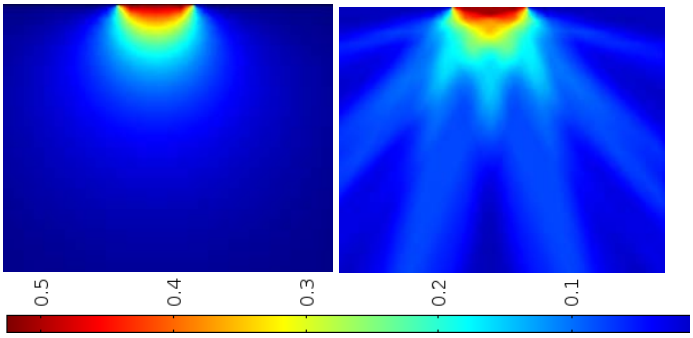

Figure 12 Steady State Hotspot Temperature Profiles (a) Kn=0.001 (b) Kn = 10

V. CONCLUSION

This paper presented COMSOL as a tool to solve the BTE and validated the results for specular/diffuse and thermalizing boundary conditions. The model was used to study the effect of local hotspots. These results can be used to predict the transport regime and hence influence the design of experiments and/or modelling methods (Fourier, BTE, molecular dynamics) based on the characteristic length scales. It was found that for Si at 300K, thermal transport can be modelled using Fourier's law if the device length is greater than 10 μm. Future work will include the transient effects and integration with the Heat Transfer module to give heat flux boundary conditions to model the hotspots more accurately. It should also be possible to include multiple hotspots and optimize their horizontal spacing.

VI. ACKNOWLEDGEMENTS

We would like to extend our thanks to Dr. Tim Fisher and Dr. Amy Marconnet for their guidance during the course of this project. We would also like to thank Dr. Anurag Kumar, Ishan Shrivastava , Collier Miers, Sina Hamian (Univeristy of Utah – Salt Lake city), Dr. Sangowook Sihn (University of Ohio – Dayton), and the COMSOL support services.

VII. REFERENCES

[1] Smith, ANDREW N., and PAMELA M. Norris. "Microscale heat transfer."*Heat Transfer Handbook* (2003): 1309-1357

[2] Murthy, Jayathi Y., et al. "Review of multiscale simulation in submicron heat transfer." *International Journal for Multiscale Computational Engineering* 3.1 (2005)

[3] Tien, Majumdar. "Gerner,"MicroscaleEnergy Transport"." (1998): 1-94

[4] Chen, Gang. "Nanoscale energy transport and conversion." (2005): 180-185

[5] Fisher, Timothy S. Thermal energy at the nanoscale. World Scientific, 2014

[6] http://www.allegromicro.com/en/Design-Center/Technical-Documents/Hall-Effect-Sensor-IC-Publications/Allegro-Hall-Effect-Sensor-ICs.aspx

[7] Joshi, A. A., and A. Majumdar. "Transient ballistic and diffusive phonon heat transport in thin films." *Journal of Applied Physics* 74.1 (1993): 31-39

[8] Chen, Guodong. *Thermal and Mechanical Behavior of Nano-structured Materials*. Diss. Case Western Reserve University, 2012

[9] Sihn, Sangwook, and Ajit K. Roy. *Nanoscale Heat Transfer using Phonon Boltzmann Transport Equation*. AIR FORCE RESEARCH LAB DAYTON OH, 2009

[10] Modest, Michael F. *Radiative heat transfer*. Academic press, 2013

[11] Lee, C. E.: "The discrete S_n approximation to transport theory," Technical Information Series Report LA2595, Lawrence Livermore Laboratory, 1962

[12] Lathrop, K. D., and B. G. Carlson: "Discrete-ordinates angular quadrature of the neutron transport equation,"Technical Information Series Report LASL-3186, Los Alamos Scientific Laboratory, 1965

[13] Fiveland, W. A.: "Discrete ordinate methods for radiative heat transfer in isotropically and anisotropically scattering media," ASME Journal of Heat Transfer, vol. 109, pp. 809–812, 1987

[14] Truelove, J. S.: "Discrete-ordinate solutions of the radiation transport equation," ASME Journal of Heat Transfer, vol. 109, no. 4, pp. 1048–1051, 1987

[15] Multiphysics, Comsol. "Heat transfer module." *User's Guide, Version* 3 (2006)

[16] Hamian, Sina, et al. "Finite element analysis of transient ballistic–diffusive phonon heat transport in two-dimensional domains." *International Journal of Heat and Mass Transfer* 80 (2015): 781-788.